Preparation and control of a cavity-field state through an atom–driven-field interaction: Towards long-lived mesoscopic states

C. J. Villas-Bôas, F. R. de Paula, R. M. Serra, and M. H. Y. Moussa
Departamento de Física, Universidade Federal de São Carlos, P.O. Box 676, São Carlos, 13565-905, São Paulo, Brazil
(Received 3 July 2003; published 20 November 2003)

The preparation of mesoscopic states of radiation and matter fields through atom-field interactions has been achieved in recent years and employed for a range of striking applications in quantum optics. Here we present a technique for the preparation and control of a cavity mode which, in addition to interacting with a two-level atom, is simultaneously submitted to linear and parametric amplification processes. The role of the amplification-controlling fields in the achievement of real mesoscopic states is to produce highly squeezed field states and, consequently, to increase both (i) the distance in phase space between the components of the prepared superpositions and (ii) the mean photon number of such superpositions. When the squeezed superposition states are submitted to the action of similarly squeezed reservoirs, we demonstrate that under specific conditions the decoherence time of the states becomes independent of both the distance in phase space between their components and their mean photon number. An explanation is presented to support this remarkable result, together with a discussion of the experimental implementation of our proposal. We also show how to produce number states with fidelities higher than those derived as circular states.

DOI: 10.1103/PhysRevA.68.053808 PACS number(s): 42.50.Ct, 42.50.Dv

I. INTRODUCTION

The successful manipulation of atom-field interactions in cavity quantum electrodynamics (QED) and trapped ions is a great achievement of present-day physics which has encouraged outstanding theoretical proposals and experimental implementations. As high-Q cavities [1] and ionic traps [2] have permitted the preparation of coherent-state superpositions of the form $|\Psi\rangle=(|\alpha e^{i\phi}\rangle+|\alpha e^{-i\phi}\rangle)/\sqrt{2}$, with mean numbers of photon and phonon quanta $|\alpha|^2\approx 10$, mesoscopic quantum coherence has been investigated. In the cavity QED domain, the progressive decoherence of mesoscopic superpositions involving radiation fields with classically distinct phases was observed through atom-field interaction [1] and the reversible decoherence of such a mesoscopic-field state has been conjectured [3]. Moreover, the generation and detection of Fock states of the radiation field was demonstrated experimentally [4], and the Rabi oscillation of circular Rydberg atoms in the vacuum and in small coherent fields in a high-Q cavity was measured [5], revealing the quantum nature of the radiation field [6].

Parallel to the achievements in cavity QED, the mastery of techniques to manipulate electronic and motional states of trapped ions with classical fields has enabled the control of fundamental quantum phenomena at a level that seems to herald a new phase in technology. The operation of a two-bit controlled-NOT quantum logic gate was demonstrated by storing the two quantum bits in the internal and external degrees of freedom of a single trapped ion [7]. A ''Schrödinger cat'' superposition of spatially separated coherent harmonic states was generated [2], as well as other nonclassical states at the single-atom level [8]. The reconstruction of the density matrices and Wigner functions of various quantum states of motion of a harmonically bound ion was also reported [9].

In addition to the atom-field interaction in cavity QED and trapped ions, the preparation of *reference* traveling-field states needed to measure the properties of *signal* traveling fields [10] has been suggested based on optical linear [11] and nonlinear devices [12]. The techniques developed over recent decades for the processes of parametric up- and down-conversion have enabled great advances in the domain of traveling waves. The production of true entanglement by type-II noncollinear phase matching in parametric down-conversion was employed to demonstrate a violation of Bell's inequality with two-photon fringe visibilities in excess of 97% [13]. Three-photon Greenberger-Horne-Zeilinger entanglement has also been observed [14], and it is worth stressing that experimental implementations of teleportation have been achieved with traveling-wave techniques [15], as these provide the facilities for preparation of the state to be teleported, for the quantum channel, and for the accomplishment of the required Bell-type measurements. High-fidelity teleportation of superpositions [16] and entanglements of running-wave field states [17] have also been presented.

As the techniques for generating nonclassical superposition states have been improved, attention has turned to a major problem that must be overcome in the contexts of quantum communication [18] and computation [19]: the decoherence of quantum states due to the inevitable coupling of the quantum systems to their environment [20–22] and even due to fluctuation in the interaction parameters required to prepare a coherent superposition [23,24]. Schemes for inhibiting decoherence by engineering the reservoir have been developed for trapped ions [25,26] and atomic two-level systems [27,28]. Measurements of the decoherence of superposed motional states of a trapped ion coupled to an engineered reservoir, where the coupling and the state of the environment are controllable [29], have also been reported. The possibility of controlling the decoherence mechanism is crucial to the preparation of the long-lived macroscopic superposition states and entanglements of macroscopic objects required for the implementation of the potential applications

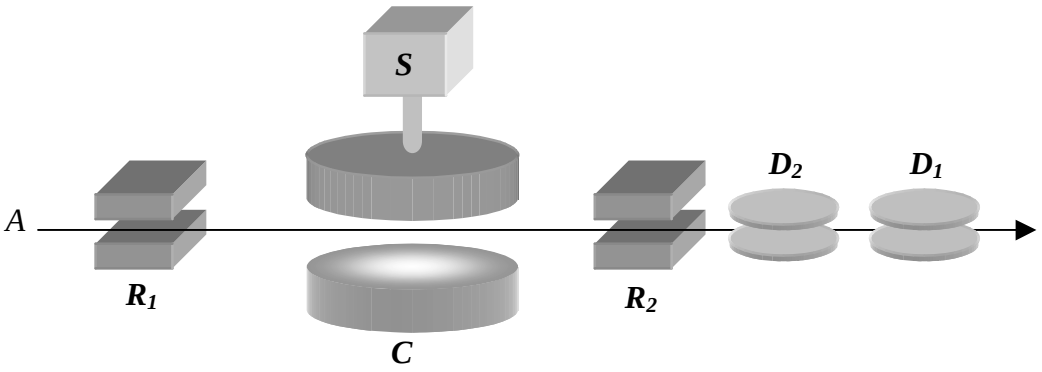

FIG. 1. Sketch of the experimental setup for atom–driven-field interaction.

of quantum mechanics in communication and computation [30]. Beyond the efforts being made to engineer mesoscopic superpositions and entanglements with photon and phonon quanta, referred to above, the possibility of engineering such mesoscopic states with massive objects has been and is being pursued. Recently, correlations (on average) of collective spin states of two macroscopic objects, each consisting of a cesium gas sample with about 10^{12} atoms, was demonstrated experimentally. In Ref. [31] an experimental scenario designed to reduce dramatically the decoherence rate of a quantum superposition of Bose-Einstein condensates is outlined. This is also our concern in the present work, focusing on the preparation of long-lived states of the radiation field in cavity QED.

Methods for manipulating cavity-field states through atoms driven by external fields [32] constitute an important means of attaining arbitrary control of a quantum field. Although the time evolution of a field state under linear and parametric amplifications has been a major concern in quantum optics for generating squeezed states and investigating their properties [33,34], classical driving fields have barely been considered for quantum states engineering purposes. Here we present a proposal for achieving long-lived mesoscopic superposition states of the radiation field in cavity QED that relies on two basic requirements: parametric amplification and an engineered squeezed-vacuum reservoir for cavity-field states (we note that the required engineered reservoir—resulting from the standard vacuum for cavity modes plus additional interactions—must be an optimum squeezed-vacuum reservoir). In addition, our technique can be employed to prepare number states with fidelities higher than those generated as circular states [35].

Our proposal considers the dispersive interaction of a two-level atom with a cavity field which is simultaneously under amplification processes. Parametric amplification is employed to achieve a high degree of squeezing and excitation of what we actually want to be a mesoscopic superposition state. We show that the prepared squeezed-mesoscopic state, under the action of a similarly squeezed reservoir, exhibits a decoherence time orders of magnitude longer than those of nonsqueezed cavity-field states subjected to the influence of (i) a squeezed reservoir and (ii) a nonsqueezed reservoir. In fact, the computed decoherence time turns out to be independent of both the average photon number and the distance in phase space between the centers of the quasiprobability distribution of the individual states composing the prepared superposition. The decoherence time depends only on the excitation of the initial coherent state injected into the cavity previous to the preparation of the squeezed superposition. This remarkable result follows when the direction of squeezing of the superposition state is perpendicular to that of the reservoir modes. Under this condition, the entanglement between the prepared state and the modes of the reservoir is minimized and so the noise injected from the reservoir into the prepared cavity mode is minimal, making it a long-lived superposition state.

We finally stress that a scheme has been presented in Ref. [36] for the implementation of parametric amplification of an arbitrary radiation-field state previously prepared in a high-Q cavity. As squeezed light is mainly supplied by nonlinear optical media as running waves (through backward [37] or forward [38] four-wave mixing and parametric down-conversion [39]), standing squeezed fields in high-Q cavities or ion traps can be generated through atom-field interaction [40]. Although considerable space has been devoted in the literature to the squeezing process in the Jaynes-Cumming model, the issue of squeezing any desired prepared cavity-field state $|\Psi\rangle$, i.e., the accomplishment of the operation $S(\zeta)|\Psi\rangle$ in cavity QED (ζ standing for a set of group parameters), has not been addressed. Engineering such an operation was the subject of Ref. [36]; it is achieved through the dispersive interactions of a three-level atom simultaneously with a classical driving field and a cavity mode whose prepared state we wish to squeeze. In short, the dispersive interaction of the cavity mode with a driven atom produces the desired operation $S(\zeta)|\Psi\rangle$. Since linear amplification is easily accomplished in cavity QED [41,42], the scheme in Ref. [36] contributes crucially for the experimental feasibility of the present proposal for preparation and control of a long-lived cavity-field state through atom–driving–field interaction.

II. ATOM–DRIVEN-FIELD INTERACTION

The proposed configuration for engineering driven-cavity-field states, depicted in Fig. 1, consists of a two-level Rydberg atom A which crosses a Ramsey-type arrangement, i.e., a high-Q micromaser cavity C located between two Ramsey

zones R_1 and R_2. After interacting with this arrangement, the atom is counted by detection chambers D_2 and D_1 (for ionizing the excited $|1\rangle$ and ground $|0\rangle$ states, respectively), projecting the cavity field in the desired state. The transition of the two-level atom A from excited to ground state is far from resonant with the cavity mode frequency, allowing a dispersive atom-field interaction to occur. In addition to the dispersive interaction with the two-level atom, the cavity mode is simultaneously submitted to linear and parametric amplifications (both represented in Fig. 1 by the source S) so that the Hamiltonian of our model (for $\hbar=1$) is given by

$$H=\omega a^{\dagger}a+\frac{\omega_0}{2}\sigma_z+\chi a^{\dagger}a\sigma_z+\mathcal{H}_{amplification}, \qquad (1)$$

where $\sigma_z=|1\rangle\langle 1|-|0\rangle\langle 0|$, $a^{\dagger}$ and a are, respectively, the creation and annihilation operators for the cavity mode of frequency ω which lies between the two atomic energy levels, which are separated by ω_0, such that the detuning $\delta=|\omega-\omega_0|$ is large enough to enable only virtual transitions to occur between the states $|0\rangle$ and $|1\rangle$. The atom-field coupling parameter inside the cavity is $\chi=\Omega^2/\delta$, where Ω is the Rabi frequency. The expression for the atom-field dispersive interaction on the right-hand side (RHS) of Eq. (1) is valid under the assumption that $\Omega^2 n\ll\delta^2+\gamma^2$, where n is a characteristic photon number and γ is the spontaneous-emission rate [43]. We suppose, for simplicity, that the atom-field coupling is turned on (off) suddenly at the instant the atom enters (leaves) the cavity region**,** such that $\chi=0$ when the atom is outside the cavity.

We consider the atom, prepared at time t_0 by the Ramsey zone R_1 in a $|0\rangle,|1\rangle$ superposition, to reach C at time t_1 and leave it at t_2. The linear and parametric pumpings are assumed to be turned on also at t_0 and turned off at a convenient time $t\geqslant t_2$. Finally, the action of the classical amplification mechanism on the cavity mode is described by the Hamiltonian

$$\mathcal{H}_{amplification}=\zeta(t)a^{\dagger 2}+\zeta^*(t)a^2+\xi(t)a^{\dagger}+\xi^*(t)a, \qquad (2)$$

where the time-dependent (TD) functions $\zeta(t)$ and $\xi(t)$ allow the parametric and linear amplifications, respectively. It is well understood that for specific values of these TD functions the eigenstates of the Schrödinger equation may squeeze the variance in one of the cavity mode's two quadrature phases [33,34,44–46].

The Schrödinger state vector associated with Hamiltonian (1) can be written using

$$|\Psi(t)\rangle=e^{i\omega_0 t/2}|0\rangle|\Phi_0(t)\rangle+e^{-i\omega_0 t/2}|1\rangle|\Phi_1(t)\rangle, \qquad (3)$$

where $|\Phi_\ell(t)\rangle=\int(d^2\alpha/\pi)\mathcal{A}_\ell(\alpha,t)|\alpha\rangle$, $\ell=0,1$, the complex quantity α standing for the eigenvalues of a, and $\mathcal{A}_\ell(\alpha,t)=\langle\alpha,\ell|\Psi(t)\rangle$ are the expansion coefficients for $|\Phi_\ell(t)\rangle$ in the coherent-state basis $\{|\alpha\rangle\}$. Using the orthogonality of the atomic states and Eqs. (1) and (3) we obtain the uncoupled TD Schrödinger equations:

$$i\frac{d}{dt}|\Phi_\ell(t)\rangle=\mathbf{H}_\ell|\Phi_\ell(t)\rangle, \qquad (4)$$

$$\mathbf{H}_\ell=\omega_\ell(t)a^{\dagger}a+\zeta(t)a^{\dagger 2}+\zeta^*(t)a^2+\xi(t)a^{\dagger}+\xi^*(t)a, \qquad (5)$$

with $\omega_\ell(t)=[\omega-(-1)^\ell\chi\Theta(t-t_1)\Theta(t_2-t)]$. Note that the problem has been reduced to that of a cavity field, under parametric and linear pumping, whose frequency ω is shifted by $-\chi$ $(+\chi)$ when interacting with the atomic state 0 (1), during the time interval $\tau=t_2-t_1$.

Solving Eq. (4) we obtain, from an initial state of the cavity mode at time t_i, $|\Phi_\ell(t_i)\rangle$, the evolved state

$$|\Phi_\ell(t)\rangle=\mathbb{U}_\ell(t,t_i)|\Phi_\ell(t_i)\rangle, \qquad (6)$$

which defines the evolution operator we are looking for. Evidently, the evolution operators $\mathbb{U}_\ell(t_1,t_0)$ and $\mathbb{U}_\ell(t,t_2)$, giving the evolution of the state vector of the radiation field while the atom is outside the cavity, do not depend on the state of the two-level atom, the label ℓ being unnecessary. However, the operator $\mathbb{U}_\ell(t_2,t_1)$, which gives the evolution of the cavity-field state during its interaction with the atom, does depend on the atomic state and differs from the operators $\mathbb{U}(t_1,t_0)$ and $\mathbb{U}(t,t_2)$ only by the shifted frequency $\omega_\ell(t)$.

III. SOLVING THE SCHRÖDINGER EQUATION VIA TIME-DEPENDENT INVARIANTS

The Hamiltonian in Eq. (5) has been investigated in the search for squeezed states of the radiation field. Group-theory methods [44,47] and TD invariants [45] have been used in attempts to solve this TD quadratic Hamiltonian, which may represent a charged particle subjected to a harmonic motion, immersed in a TD uniform magnetic field, a single-mode photon field traveling through a squeezing medium or, as in the present situation, a cavity mode with shifted frequency under linear and parametric amplification. In the present work, we make use of the TD invariants of Lewis and Riesenfeld [48] to solve the Schrödinger equation (4), following the reasoning in Ref. [45]: instead of proposing an invariant associated with the Hamiltonian (5), we first perform a unitary transformation on Eq. (4) in order to reduce it to a form which already has a known associated invariant. Thus, under a unitary transformation represented by the operator $S(\varepsilon_\ell)$ (ε_ℓ standing for a set of TD group parameters which may also depend on the atomic state ℓ), we obtain from Eq. (4)

$$i\frac{d}{dt}|\Phi_\ell^S(t)\rangle=\mathcal{H}_\ell^S|\Phi_\ell^S(t)\rangle, \qquad (7)$$

where the transformed Hamiltonian and wave vector are given by

$$\mathcal{H}_\ell^S=S^{\dagger}(\varepsilon_\ell)\mathbf{H}_\ell S(\varepsilon_\ell)+i\frac{dS^{\dagger}(\varepsilon_\ell)}{dt}S(\varepsilon_\ell), \qquad (8a)$$

$$|\Phi_\ell^S(t)\rangle = S^\dagger(\varepsilon_\ell)|\Phi_\ell(t)\rangle. \tag{8b}$$

In what follows we employ two theorems to obtain the solution of the TD Schrödinger equation (4): (a) a theorem expounded in [45] asserts that if $I_\ell(t)$ is an invariant associated with $\mathbf{H}_\ell$ (i.e., $dI_\ell(t)/dt = \partial I_\ell/\partial t + i[\mathcal{H}_\ell, I_\ell(t)] = \mathbf{0}$), then the transformed operator $I_\ell^S(t) = S^\dagger(\varepsilon_\ell) I_\ell(t) S(\varepsilon_\ell)$ will be an invariant associated with $\mathcal{H}_\ell^S$; (b) on the other hand, from Lewis and Riesenfeld's well-known theorem [48], it follows that a solution of the Schrödinger equation is an eigenstate of the Hermitian invariant $I_\ell(t)$ multiplied by a TD phase factor. It follows from (a) and (b) that the solutions of Eq. (4) are given by

$$\begin{aligned}|\Phi_{\ell,m}(t)\rangle &= S(\varepsilon_\ell)|\Phi_{\ell,m}^S(t)\rangle \\ &= S(\varepsilon_\ell) e^{i\phi_{\ell,m}^S(t)}|m,t\rangle_S, \quad m = 0,1,2,\ldots,\end{aligned} \tag{9}$$

where $|m,t\rangle_S$ is the eigenstate of the invariant [49] and the Lewis and Riesenfeld phase [48] obeys

$$\phi_{\ell,m}^S(t) = \int_{t_i}^t dt'\, {}_S\langle m,t'|\left(i\frac{\partial}{\partial t'} - \mathcal{H}_\ell^S\right)|m,t'\rangle_S. \tag{10}$$

It is straightforward to verify that under the unitary transformation carried out by the operator $S(\varepsilon_\ell)$ the TD phase is invariant: $\phi_{\ell,m}^S(t) = \phi_{\ell,m}(t)$.

A. The transformed Hamiltonian

Next, we associate the unitary transformation with the squeeze operator $S(\varepsilon_\ell) = \exp[\frac{1}{2}(\varepsilon_\ell a^{\dagger 2} - \varepsilon_\ell^* a^2)]$, where the complex TD function $\varepsilon_\ell = r_\ell(t) e^{i\varphi_\ell(t)}$ includes the squeeze parameters $r_\ell(t)$ and $\varphi_\ell(t)$. $r_\ell(t)$ is associated with a squeeze factor, while $\varphi_\ell(t)$ defines the squeezing direction in phase space. Moreover, the TD parameters for the parametric and linear amplification processes are written as $\zeta(t) = \kappa(t) e^{i\eta(t)}$ and $\xi(t) = \varkappa(t) e^{i\varpi(t)}$, respectively. The squeeze parameters $(r_\ell(t), \varphi_\ell(t))$, the amplification amplitudes $(\kappa(t), \varkappa(t))$, and frequencies $(\eta(t), \varpi(t))$ are all real TD functions. With the above assumptions and after a lengthy calculation, the transformed Hamiltonian becomes

$$\mathcal{H}_\ell^S = \Omega_\ell(t) a^\dagger a + \Lambda_\ell(t) a^\dagger + \Lambda_\ell^*(t) a + \mathsf{F}_\ell(t), \tag{11}$$

provided that its TD coefficients satisfy

$$\Omega_\ell(t) = \omega_\ell(t) + 2\kappa(t) \tanh r_\ell(t) \cos[\eta(t) - \varphi_\ell(t)], \tag{12a}$$

$$\Lambda_\ell(t) = \xi(t) \cosh r_\ell(t) + \xi^*(t) e^{i\varphi_\ell(t)} \sinh r_\ell(t), \tag{12b}$$

$$\mathsf{F}_\ell(t) = \kappa(t) \tanh r_\ell(t) \cos[\eta(t) - \varphi_\ell(t)], \tag{12c}$$

while the squeeze parameters $r_\ell(t)$ and $\varphi_\ell(t)$ are determined by solving the coupled differential equations

$$\dot{r}_\ell(t) = 2\kappa(t) \sin[\eta(t) - \varphi_\ell(t)], \tag{13a}$$

$$\dot{\varphi}_\ell(t) = -2\omega_\ell(t) - 4\kappa(t) \coth[2r_\ell(t)] \cos[\eta(t) - \varphi_\ell(t)]. \tag{13b}$$

It is evident from these relations that the TD group parameters $\varepsilon_\ell(t)$, defining the unitary operator $S(\varepsilon_\ell)$, depend on the atomic state ℓ, as assumed from the beginning. We finally mention that we have associated the unitary transformation with the squeeze operator since the parametric amplification described by Hamiltonian (2) actually squeezes the cavity-field state. In fact, the TD parameter $\zeta(t)$ allowing the parametric amplification in Eq. (2) is connected to the squeeze parameters $(r_\ell(t), \varphi_\ell(t))$ as expressed by Eqs. (13a) and (13b).

B. The evolution operators

With the Hamiltonian (11) at hand we return to the solution of the Schrödinger equation (7). The application of the invariant method leads to the wave vector [49]

$$|\Phi_{\ell,m}^S(t)\rangle = e^{i\phi_{\ell,m}(t)} D[\theta_\ell(t)]|m\rangle, \quad m = 0,1,2,\ldots, \tag{14}$$

where $|m\rangle$ is the number state and $D[\theta_\ell(t)] = \exp[\theta_\ell(t) a^\dagger - \theta_\ell^*(t) a]$ is the displacement operator, $\theta_\ell(t)$ being a solution to the equation $i\dot{\theta}_\ell(t) = \Omega_\ell(t)\theta_\ell(t) + \Lambda_\ell(t)$, given by

$$\theta_\ell(t) = e^{-i\beta_\ell(t)}\left(\theta_\ell(t_i) - i\int_{t_i}^t \Lambda_\ell(t') e^{i\beta_\ell(t')} dt'\right), \tag{15}$$

with $\beta_\ell(t) = \int_{t_i}^t \Omega_\ell(t') dt'$. We note that $\theta_\ell(t_0)$ describes the initial cavity-field state which will be assumed to be a coherent state $|\alpha\rangle$, the subscript ℓ being purely formal. From the substitution of Hamiltonian (11) into the Lewis and Riesenfeld phase, defined in Eq. (10), we obtain

$$\begin{aligned}\phi_{\ell,m}(t) = -\int_{t_i}^t \Big\{ & m\Omega_\ell(t') + \frac{1}{2}[\Lambda_\ell^*(t')\theta_\ell(t') \\ & + \Lambda_\ell(t')\theta_\ell^*(t')] + \gamma_\ell(t') \Big\} dt'.\end{aligned} \tag{16}$$

Therefore, the solutions of the Schrödinger equation (4), which form a complete set, can be written

$$|\Phi_{\ell,m}(t)\rangle = S[\varepsilon_\ell(t)]|\Phi_{\ell,m}^S(t)\rangle = U_\ell(t)|m\rangle, \tag{17}$$

where

$$U_\ell(t) = \Upsilon_\ell(t) S[\varepsilon_\ell(t)] D[\theta_\ell(t)] R[\Omega_\ell(t)] \tag{18}$$

is a unitary operator containing, in addition to the squeezed and the displacement operators, a global phase factor

$$\Upsilon_\ell(t) = \exp\left\{-i\int_{t_i}^t [\mathrm{Re}[\Lambda_\ell^*(t')\theta_\ell(t')] + \mathsf{F}_\ell(t')] dt'\right\}. \tag{19}$$

The rotation operator in phase space, derived from the TD Lewis and Riesenfeld phase factor, is given by

$$R[\Omega_\ell(t)]=\exp[-ia^\dagger a\beta_\ell(t)] \tag{20}$$

Hence, for the solution of Schrödinger equation (4), we find

$$\begin{aligned}|\Phi_\ell(t)\rangle&=\sum_{m=0}^{\infty} C_m|\Phi_{\ell,m}(t)\rangle\\&=U_\ell(t)\sum_{m=0}^{\infty} C_m|m\rangle\\&=U_\ell(t)U_\ell^\dagger(t_i)|\Phi_\ell(t_i)\rangle,\end{aligned} \tag{21}$$

which finally defines the evolution operators

$$\mathbb{U}_\ell(t,t_i)=U_\ell(t)U_\ell^\dagger(t_i). \tag{22}$$

We note that for the initial time $R[\Omega_\ell(0)]=R[0]=\mathbf{1}$, $D[\theta_\ell(0)]=D[\alpha]$, $S[\varepsilon_\ell(0)]=S[0]=\mathbf{1}$, and $\Upsilon_\ell(0)=1$.

IV. EVOLUTION OF THE ATOM-FIELD STATE

Let us assume that the micromaser cavity is prepared at time t_0 in a single-mode coherent state $|\alpha\rangle$ by a monochromatic source, such that with $m=0$ in Eq. (17) we have $\theta_\ell(t_0)=\alpha$. Classical microwave fields are injected into the cavity and the amplitudes of these fields can be adjusted by varying the injection time. As mentioned above, the linear and parametric pumping are supposed to be turned on, also at t_0, the same time the atom is prepared by the Ramsey zone R_1 in the superposition state $c_0|0\rangle+c_1|1\rangle$. The combined atom-field state at the initial time t_0 is, from Eq. (3),

$$|\Psi(t_0)\rangle=[e^{i\omega_0 t_0/2}c_0|0\rangle+e^{-i\omega_0 t_0/2}c_1|1\rangle]|\alpha\rangle. \tag{23}$$

In fact, with $\mathcal{A}_\ell(\beta,t_0)=\langle\beta,\ell|(c_0|0\rangle+c_1|1\rangle)|\alpha\rangle$ it follows immediately that $|\Phi_\ell(t_0)\rangle=\int(d^2\beta/\pi)\mathcal{A}_\ell(\beta,t_0)|\beta\rangle=c_\ell|\alpha\rangle$.

The evolution of the initial state $|\Psi(t_0)\rangle$ to the time the atom reaches the cavity reads

$$|\Psi(t_1)\rangle=\mathbb{U}(t_1,t_0)|\Psi(t_0)\rangle. \tag{24}$$

Evidently, the evolution operators $\mathbb{U}(t_1,t_0)$ and $\mathbb{U}(t,t_2)$, which govern the dynamics of the cavity-field state while the atom is outside the cavity, do not depend on the state of the two-level atom. On the other hand, during the time interval $\tau=t_2-t_1$ the atom spends inside the cavity the evolution of the entire system is dictated by the operator $\mathbb{U}_\ell(t_2,t_1)=U_\ell(t_2)U_\ell^\dagger(t_1)$. This depends on the atomic state ℓ and differs from the operators $\mathbb{U}(t_1,t_0)$ and $\mathbb{U}(t,t_2)$ by the shifted frequency $\omega_\ell(t)$. Therefore, at the time the atom leaves the cavity, the state of the atom-field system is given by

$$\begin{aligned}|\Psi(t_2)\rangle=&[e^{i\omega_0 t_2/2}c_0|0\rangle\mathbb{U}_0(t_2,t_1)\\&+e^{-i\omega_0 t_2/2}c_1|1\rangle\mathbb{U}_1(t_2,t_1)]\mathbb{U}(t_1,t_0)|\alpha\rangle.\end{aligned} \tag{25}$$

After crossing the cavity, the atom evolves freely from t_2 until the time it reaches the second Ramsey zone R_2. During this time interval, the cavity mode continues to be pumped and the complete state of the system, evolving under the operator $\mathbb{U}(t,t_2)$, reads

$$\begin{aligned}|\Psi(t)\rangle=&\mathbb{U}(t,t_2)[e^{i\omega_0 t/2}c_0|0\rangle\mathbb{U}_0(t_2,t_1)\\&+e^{-i\omega_0 t/2}c_1|1\rangle\mathbb{U}_1(t_2,t_1)]\mathbb{U}(t_1,t_0)|\alpha\rangle.\end{aligned} \tag{26}$$

Next, the atom crosses the Ramsey zone R_2, where a $\pi/2$ pulse is applied, leading the atom-field system to the entangled state

$$\begin{aligned}|\Psi(t)\rangle=&\frac{1}{\sqrt{2}}\{[-e^{i\omega_0 t/2}c_0\mathsf{U}_0(t,t_0)+e^{-i\omega_0 t/2}c_1\mathsf{U}_1(t,t_0)]|0\rangle\\&+[e^{i\omega_0 t/2}c_0\mathsf{U}_0(t,t_0)+e^{-i\omega_0 t/2}c_1\mathsf{U}_1(t,t_0)]|1\rangle\}|\alpha\rangle,\end{aligned} \tag{27}$$

where we have defined the operators

$$\mathsf{U}_\ell(t,t_0)=\mathbb{U}(t,t_2)\mathbb{U}_\ell(t_2,t_1)\mathbb{U}(t_1,t_0). \tag{28}$$

Finally, measurement of the atomic state projects the cavity field into the "Schrödinger cat"–like state

$$|\Psi(t)\rangle=\mathcal{N}_\pm[\pm e^{i\omega_0 t/2}c_0\mathsf{U}_0(t,t_0)+e^{-i\omega_0 t/2}c_1\mathsf{U}_1(t,t_0)]|\alpha\rangle, \tag{29}$$

where the sign $+$ or $-$ occurs if the atom is detected in state $|1\rangle$ or $|0\rangle$, respectively, and $\mathcal{N}_\pm$ refers to the normalization factors. From Eq. (29) it follows that, after measuring the atomic level used to generate the superposition state of the radiation field, it is possible to control this superposition by adjusting the TD amplification parameters $\kappa(t)$, $\varkappa(t)$, $\eta(t)$, and $\varpi(t)$.

It is worth noting that expression (29) can be manipulated, employing Eqs. (28), (22), and Eq. (18), to give the simple form

$$\begin{aligned}|\Psi(t)\rangle&=\mathcal{N}_\pm[\pm e^{i\omega_0 t/2}c_0\Upsilon_0(t)S[\varepsilon_0(t)]|\theta_0(t)\rangle\\&\quad+e^{-i\omega_0 t/2}c_1\Upsilon_1(t)S[\varepsilon_1(t)]|\theta_1(t)\rangle]\\&=\mathcal{N}_\pm\sum_{\ell=0}^{1} c_\ell(t)S[\varepsilon_\ell(t)]D[\theta_\ell(t)]|0\rangle\\&=\mathcal{N}_\pm\sum_{\ell=0}^{1} c_\ell(t)S[\varepsilon_\ell(t)]|\theta_\ell(t)\rangle,\end{aligned} \tag{30}$$

where $c_\ell(t)=\pm(\pm)^\ell e^{(-)^\ell i\omega_0 t/2}c_\ell\Upsilon_\ell(t)$ and the amplitude of the coherent state $|\theta_\ell(t)\rangle$ follows from Eq. (15).

Passing N atoms through the cavity

Let us proceed to the construction of a cavity-field state by passing two or more atoms through cavity C. It is easy to conclude from Eq. (29) that, after the passage of N atoms through cavity C, each atom prepared in the state $c_{0,k}|0\rangle+c_{1,k}|1\rangle$ by R_1, $k=1,\ldots,N$, we obtain the cavity-field state

$$|\Psi_N(t)\rangle = \mathcal{N}_{\pm}\prod_{k=1}^{N}\left[\pm e^{i\omega_0 t/2}c_{0,k}\mathsf{U}_{0,k}(t_{f,k},t_{i,k}) + e^{-i\omega_0 t/2}c_{1,k}\mathsf{U}_{1,k}(t_{f,k},t_{i,k})\right]|\alpha\rangle, \tag{31}$$

where $t_{i,k}$ stands for the time when the kth atom is prepared by R_1 and $t_{f,k}$ stands for the time when the kth atom is detected, assumed to be the same as $t_{i,k+1}$. Therefore, we obtain

$$\mathsf{U}_{\ell,k}(t_{f,k},t_{i,k}) = \mathbb{U}(t_{f,k}=t_{i,k+1},t_{2,k}) \times \mathbb{U}_{\ell}(t_{2,k},t_{1,k})\mathbb{U}(t_{1,k},t_{i,k}=t_{f,k-1}).$$

After some manipulation and using Eq. (30), the state (31) can be simplified to the form

$$|\Psi_N(t)\rangle = \mathcal{N}_{\pm}\sum_{\ell_1,\ldots,\ell_N=1}^{2}\prod_{k=1}^{N}c_{\ell_k}(t)S[\varepsilon_{\ell_1,\ldots,\ell_N}(t)] \times|\theta_{\ell_1,\ldots,\ell_N}(t)\rangle$$

$$= \mathcal{N}_{\pm}\sum_{k=1}^{2^N}C_k(t)S[\Xi_k(t)]|\vartheta_k(t)\rangle, \tag{32}$$

where we have replaced $\Sigma_{\ell_1,\ldots,\ell_N=1}^{2}$ by $\Sigma_{k=1}^{2^N}$, i.e., $\Xi_k(t)\equiv r_{\ell_1,\ldots,\ell_N}(t)\exp[i\varphi_{\ell_1,\ldots,\ell_N}(t)]$ and $\vartheta_k(t)\equiv\theta_{\ell_1,\ldots,\ell_N}(t)$.

V. ANALYTICAL SOLUTIONS OF THE CHARACTERISTIC EQUATIONS (13A) AND (13B)

In this section we present some specific solutions of the characteristic equations (13a) and (13b), following a more detailed treatment in [45]. We investigate the situation where the cavity mode $|\alpha\rangle$ is resonant with the driving classical fields during the time the atom is out of the cavity: from t_0 to t_1 and from t_2 to t. The parametric amplifier is assumed to operate in a degenerate mode in which the *signal* and the *idler* frequencies coincide, producing a single-mode driving field. In the resonant regime this single-mode field has the same frequency ω as the cavity mode so that $\eta(t)=-2\omega t$ [33]. For the resonant linear amplifier it follows that $\varpi(t)=-\omega t$. However, during the time that the atom is inside the cavity, from t_1 to t_2, it pulls the mode frequency out of resonance with the classical driving fields, establishing a dispersive regime of the amplification process. Thus, in what follows we derive the solutions of the coupled differential equations (13a) and (13b) for the resonant and dispersive regimes.

A. Resonant amplification

We start with the solution of the characteristic equations (13a) and (13b) for the resonant amplification that operates while the atom is out of the cavity, from t_0 to t_1 and t_2 to t, when so that $\omega_\ell(t)=\omega$, $\varpi(t)=-\omega t$, and $\eta(t)=-2\omega t$. Defining $\omega=\dot{f}(t)$, $\varphi(t)=-2f(t)+g(t)$, and $\eta(t)=-2f(t)+h(t)$, Eqs. (13a) and (13b) become

$$\dot{r}(t)=-2\kappa(t)\sin[g(t)-h(t)], \tag{33a}$$

$$\dot{g}(t)=-4\kappa(t)\coth[2r(t)]\cos[g(t)-h(t)]. \tag{33b}$$

Assuming that $h(t)=h$ is a constant, the time dependence is eliminated from Eqs. (33a) and (33b) and we are left with the first-order differential equation

$$\frac{dr}{dg}=\frac{1}{2}\tanh(2r)\tan(g-h). \tag{34}$$

After integrating Eq. (34) we obtain the constant of motion

$$\cos[\varphi(t)-\eta(t)]\sinh[2r(t)]=\mathcal{C}_i, \tag{35}$$

with $\mathcal{C}_i$ depending on the initial values $r(t_i)$, $\varphi(t_i)$, and $\eta(t_i)$, where $i=0,2$. Thus, the solutions of Eqs. (33a) and (33b), which apply under the condition $\cosh^2[2r(t)]>1+\mathcal{C}_i^2$, are given by

$$\cosh[2r(t)] = \sqrt{1+\mathcal{C}_i^2}\cosh\left[\cosh^{-1}\left(\frac{\cosh 2r(t_i)}{\sqrt{1+\mathcal{C}_i^2}}\right)\pm u(t,t_i)\right], \tag{36a}$$

$$\cos[\varphi(t)-\eta(t)]=\frac{\mathcal{C}_i}{\sqrt{\cosh^2 2r(t)-1}}, \tag{36b}$$

where

$$u(t,t_i)=4\int_{t_i}^{t}\kappa(t)dt. \tag{37}$$

Note that for $t_i=0$ the $\cosh^{-1}$ term in Eq. (36a) is null, and the signals $\pm$ become irrelevant. However, for $t_i=t_2$ we choose the sign that gives $r(t)\geqslant 0$.

B. Dispersive amplification

Dispersive amplification occurs during the time the atom is inside the cavity, shifting the mode frequency ω by $\chi=\Omega^2/\delta$, so that $\omega_\ell=\omega\pm\chi$. Evidently, the amplification frequencies are unaffected by the passage of the atom, so that $\eta(t)=-2\omega t$ and $\varpi(t)=-\omega t$. Assuming that the parameter κ is time independent and defining $\varphi_\ell(t)-\eta(t)=f_\ell(t)$ and $\dot{\eta}(t)+2\omega_\ell(t)=\dot{g}_\ell$, Eqs. (13a) and (13b) become

$$\dot{r}_\ell(t)=2\kappa(t)\sin[f_\ell(t)], \tag{38a}$$

$$\dot{f}_\ell(t)=-\dot{g}_\ell-4\kappa(t)\coth[2r_\ell(t)]\cos[f_\ell(t)]. \tag{38b}$$

Since $\dot{g}_\ell=-(-1)^\ell 2\chi$ is a constant, Eqs. (38a) and (38b) can be solved by quadrature, leading to a constant of motion

$$\cosh[2r_\ell(t)]+\mathfrak{P}_\ell\cos[\varphi_\ell(t)-\eta(t)]\sinh[2r_\ell(t)]=\mathcal{C}_1, \tag{39}$$

which now depends on the initial values $r(t_1)$, $\varphi(t_1)$, and $\eta(t_1)$. Despite the assumption that the atom-field coupling is turned on (off) suddenly, these initial values must be computed from the solutions for the resonant amplification regime at time t_1. With this procedure we obtain the solutions for the resonant amplification $(r(t_1),\ \varphi(t_1))$ as the limit of those for the dispersive amplification $(r(t_1),\ \varphi(t_1))$ as $\chi\to 0$. The parameter $\mathfrak{P}_\ell=-(-1)^\ell 2\kappa/\chi$, defined for a constant amplification amplitude κ, is an effective macroscopic coupling. Therefore, for the dispersive regime, we find three different solutions, depending on whether the coupling is strong ($|\mathfrak{P}_\ell|>1$), weak ($|\mathfrak{P}_\ell|<1$), or critical ($|\mathfrak{P}_\ell|=1$).

(a)With strong coupling ($|\mathfrak{P}_\ell|>1$), we have the relations

$$\cosh[2r_\ell(t)]=\frac{1}{\mathfrak{P}_\ell^2-1}\left[\frac{e^{h(t)}}{4}+\mathfrak{P}_\ell^2(\mathcal{C}_1^2+\mathfrak{P}_\ell^2-1)e^{-h(t)}-\mathcal{C}_1\right], \tag{40a}$$

$$\cos[\varphi_\ell(t)-\eta(t)]=\frac{\mathcal{C}_1-\cosh[2r_\ell(t)]}{\mathfrak{P}_\ell\sinh[2r_\ell(t)]}, \tag{40b}$$

where

$$h(t)=\mp\frac{\sqrt{\mathfrak{P}_\ell^2-1}}{|\mathfrak{P}_\ell|}u(t,t_1)+\ln[2|\mathfrak{P}_\ell|(\sqrt{(\mathfrak{P}_\ell^2-1)(\mathcal{C}_1^2-1)}+\mathcal{C}_1|\mathfrak{P}_\ell|)], \tag{41}$$

the sign being chosen so that $r(t)\geqslant 0$. The function $u(t,t_1)$ is defined by Eq. (37).

(b) For the weak coupling regime ($|\mathfrak{P}_\ell|<1$), the TD squeeze parameters when $\mathcal{C}_1>\sqrt{1-\mathfrak{P}_\ell^2}$ are given by Eq. (40b) and

$$\cosh[2r_\ell(t)]=\frac{\mathcal{C}_1}{1-\mathfrak{P}_\ell^2}\left\{1-\frac{|\mathfrak{P}_\ell|\sqrt{\mathcal{C}_1^2+\mathfrak{P}_\ell^2-1}}{\mathcal{C}_1}\times\sin\left[\pm\frac{\sqrt{1-\mathfrak{P}_\ell^2}}{|\mathfrak{P}_\ell|}u(t,t_1)+\arcsin\left(\frac{\mathcal{C}_1|\mathfrak{P}_\ell|}{\sqrt{\mathcal{C}_1^2+\mathfrak{P}_\ell^2-1}}\right)\right]\right\}. \tag{42}$$

(c) Finally, for critical coupling ($|\mathfrak{P}_\ell|=1$), the TD squeeze parameters are given by Eq. (40b) and the solution for $r_\ell(t)$ follows from the equation

$$\cosh[2r_\ell(t)]=\frac{1}{2\mathcal{C}_1}[1+\mathcal{C}_1^2+(\sqrt{\mathcal{C}_1[2\cosh(2r(t_1)]-\mathcal{C}_1)-1}\mp\mathcal{C}_1u(t,t_1))^2], \tag{43}$$

the parameter ℓ being redundant. Note that in Eqs. (40a) and (42) the parameter ℓ is also unnecessary since the RHS of Eq. (40a) is an even function of $\mathfrak{P}_\ell$. Therefore, the squeezing factor $r(t)$ does not depend on the atomic state, in contrast to the squeezing direction in phase space defined by $\varphi_\ell(t)$.

From the above solutions for the resonant and dispersive amplifications it is straightforward to obtain the behavior of the TD squeeze parameters from time t_0, when the classical driving fields are turned on simultaneously to the preparation of the atomic state by R_1, to any instant t after, the atom-field interaction. The time t may be chosen to be before, after or in the course of the ionization detection of the atomic state.

(i) From t_0 to t_1, the squeeze parameters follow from Eqs. (36a) and (36b). As mentioned above, such equations apply under the condition $\cosh^2[2r(t)]>1+\mathcal{C}_i^2$, which is always satisfied for $\mathcal{C}_i=0$, a value following from the initial conditions $r(t_0)$, $\varphi(t_0)$, and $\eta(t_0)$. In fact, for an initial coherent state injected into the cavity: $r(t_0)=0$. Assuming the parameter κ to be time independent, together with $\mathcal{C}_0=0$, Eqs. (36a) and (36b) lead to the simplified solutions

$$r(t)=2\kappa t, \tag{44a}$$

$$\varphi(t)=-2\omega t+\pi/2. \tag{44b}$$

(ii) From t_1 to t_2 we have three possible solutions for the squeeze parameters, depending on the coupling strength $|\mathfrak{P}_\ell|$. These solutions follow from the above-described expressions, in Eqs. (40a), (40b), (42), and (43), given that the constant of motion $\mathcal{C}_1=\cosh(4\kappa t_1)$, computed from Eqs. (39), (44a), and (44b) with $t=t_1$. It is straightforward to observe in these equations the well-known threshold in the behavior of the TD squeeze factor $r(t)$, following from the quadratic TD Hamiltonian (5) [45]: $r(t)$ increases monotonically for $|\mathfrak{P}_\ell|\geqslant 1$, while for $|\mathfrak{P}_\ell|<1$ it oscillates periodically. In the present paper we are interested in the weak coupling regime, where the squeeze parameters follow from Eqs. (40b) and (42). We note that for realistic physical parameters we achieve higher squeezing factors even in this regime.

(iii) From t_2 to t the squeeze parameters are again derived from Eqs. (36a) and (36b). The constant of motion is computed from the initial conditions $r(t_2)$, $\varphi(t_2)$, and $\eta(t_2)$, which depend on the strong, critical, or weak coupling regimes. For weak coupling, $|\mathfrak{P}_\ell|<1$, in which we are interested, the constant of motion in Eq. (35), derived from Eqs. (40b) and (42) and depending on the atomic state, reads

$$\mathcal{C}_{2,\ell}=\frac{\mathcal{C}_1-\cosh[2r(t_2)]}{\mathfrak{P}_\ell}. \tag{45}$$

VI. WIGNER FUNCTIONS AND FLUCTUATIONS OF THE QUADRATURES

Now we analyze the states (30) and (32), projected into the cavity after the detection of one or several atoms, respectively, and especially control of these states through the amplification parameters. From here on we assume that the atom is detected in excited state $|1\rangle$, so that $|\Psi(t)\rangle=\mathcal{N}_+\sum_{\ell=0}^{1}c_\ell(t)S[\varepsilon_\ell(t)]|\theta_\ell(t)\rangle$ for Eq. (30) and $|\Psi(t)\rangle=\mathcal{N}_\pm\sum_{k=1}^{2^N}C_k(t)S[\Xi_k(t)]|\vartheta_k(t)\rangle$ for Eq. (32). After

computing the density operator of these cavity-field states, $\rho(t)=|\Psi(t)\rangle\langle\Psi(t)|$, which reflects all the properties of a quantum system—such as superpositions and decoherence (when fluctuating parameters are in order)—the symmetric ordered characteristic function, defined as in [33], follows:

$$\mathfrak{C}_S(\gamma,\gamma^*,t)=\mathrm{Tr}[\rho(t)e^{\gamma a^\dagger-\gamma^* a}]=\langle\Psi(t)|e^{\gamma a^\dagger-\gamma^* a}|\Psi(t)\rangle. \tag{46}$$

From the characteristic function $\mathfrak{C}_S(\gamma,\gamma^*,t)$ we define the Wigner distribution function [33]

$$W(\eta,\eta^*,t)=\frac{1}{\pi^2}\int d^2\gamma\mathfrak{C}_S(\gamma,\gamma^*,t)e^{\gamma^*\eta-\gamma\eta^*}, \tag{47}$$

which will be employed here to represent the quantum properties of the cavity-field state conveniently in a three-dimensional $\mathrm{Re}(\eta),\mathrm{Im}(\eta),W$ space. The result of the lengthy and somewhat involved integration over the entire complex plane is presented in the Appendix, only for the state (30).

Next we analyze the fluctuations of the quadratures of the cavity mode, defined as the dimensionless position and momentum operators $X_1=(a+a^\dagger)$ and $X_2=-i(a-a^\dagger)$, respectively. The dynamic fluctuations for these quadrature operators in the cavity-field state, given by

$$\langle\Delta X_j^2\rangle=\langle X_j^2\rangle-\langle X_j\rangle^2, \quad j=1,2, \tag{48}$$

are obtained by computing the variances

$$\langle\Delta a^2\rangle=\langle a^2\rangle-\langle a\rangle^2, \tag{49a}$$

$$\langle\Delta(a^\dagger)^2\rangle=\langle(a^\dagger)^2\rangle-\langle(a^\dagger)\rangle^2, \tag{49b}$$

$$\langle\Delta a^\dagger a\rangle=\langle a^\dagger a\rangle-\langle a^\dagger\rangle\langle a\rangle. \tag{49c}$$

We note that with the above definitions for X_1 and X_2 we get for the coherent state the minimum uncertainty value $\langle\Delta X_j^2\rangle=1$. The expected values of the normal ordered operators defined in Eqs. (49a), (49b), and (49c) may be conveniently evaluated with the help of the normal ordered characteristic function

$$\mathfrak{C}_N(\gamma,\gamma^*,t)=\mathrm{Tr}[\rho(t)e^{\gamma a^\dagger}e^{-\gamma^* a}]=e^{|\gamma|^2/2}\mathfrak{C}_S(\gamma,\gamma^*,t). \tag{50}$$

From this equation, if we want the normally ordered moments, it is easy to derive the expression

$$\langle(a^\dagger)^n a^m\rangle=\frac{\partial^n}{\partial\gamma^n}\frac{\partial^m}{\partial(-\gamma^*)^m}\mathfrak{C}_N(\gamma,\gamma^*,t)\bigg|_{\gamma=\gamma^*=0}, \tag{51}$$

which is suitable for computing the variances in Eqs. (49a), (49b), (49c), and (48).

VII. PROTOCOLS FOR THE PREPARATION OF "SCHRÖDINGER CAT"–LIKE STATES AND NUMBER STATES

A. "Schrödinger cat"–like states

To prepare a particular superposition state from Eq. (30) we follow a three-step protocol. (1) First, we adjust the amplitude κ of the parametric amplification and the atom-field interaction time $\tau=t_2-t_1$ in order to obtain a particular angle $\Theta=|\varphi_1(t_2)-\varphi_2(t_2)|$ defined by the squeezing directions of the states composing the "Schrödinger cat"–like superposition. (2) Next, the desired excitation of the prepared state can be achieved by manipulating the excitation of the initial coherent state injected into the cavity, the amplitude of the linear amplification (that of the parametric amplification has been fixed in the first step), and the time interval of the amplification process. (3) Finally, the amplitude of both states composing the superposition can be adjusted through the probability amplitudes of the atomic superposition state prepared in the first Ramsey zone.

In Figs. 2(a), 2(b), and 2(c) we present some superposition states of the cavity mode generated with the above protocol. In all these figures we have considered an atom prepared in R_1 in the superposition $(|0\rangle+|1\rangle)/\sqrt{2}$. We have also disregarded the linear amplification process while the parametric amplification is switched off at $t=t_2$ when the atom leaves the cavity. In the captions of Figs. 2(a), 2(b), and 2(c) we present the fluctuations for the quadrature operators and the parameters $r(t_2)$ and Θ used for the preparation of the desired states. Figures 2(a) and 2(b) indicate the possibility to control the squeezing directions of the quasiprobability distribution of the individual states composing the prepared "Schrödinger cat"–like superposition. This control will be extremely useful for generating number state as circular squeezed states as shown below.

It is worth noting that a number of exoticreference states have being requested for measuring properties of chosen field states. In Ref. [11] the reciprocal-binomial state is requested as a reference field for measuring the phase distribution of a chosen field without having to obtain sufficient information to reconstruct its complete state. An extension of the proposal in Ref. [11] was present for the *Q*-function measurement where a convenient choice of a reference state allows us to measure dispersions of quadrature operators [50]. Therefore, we hope that the control of the squeezing directions of the components of superposition states achieved through our scheme could also be employed to generate these useful reference states. We also mention that the state in Fig. 2(c), considered in the analysis in Sec. VIII, is crucial for achieving long-lived mesoscopic superposition states of the radiation field in cavity QED.

Finally, we recall that the amplification processes could be considered, after the atom-field interaction, for controlling the prepared cavity-field state. Both amplification processes can furnish excitation to the cavity mode, while the parametric one is able to increase the degree of squeezing.

B. Number states as circular squeezed states

From the present scheme of atom-driven field interaction it is possible to generate number states with higher fidelity

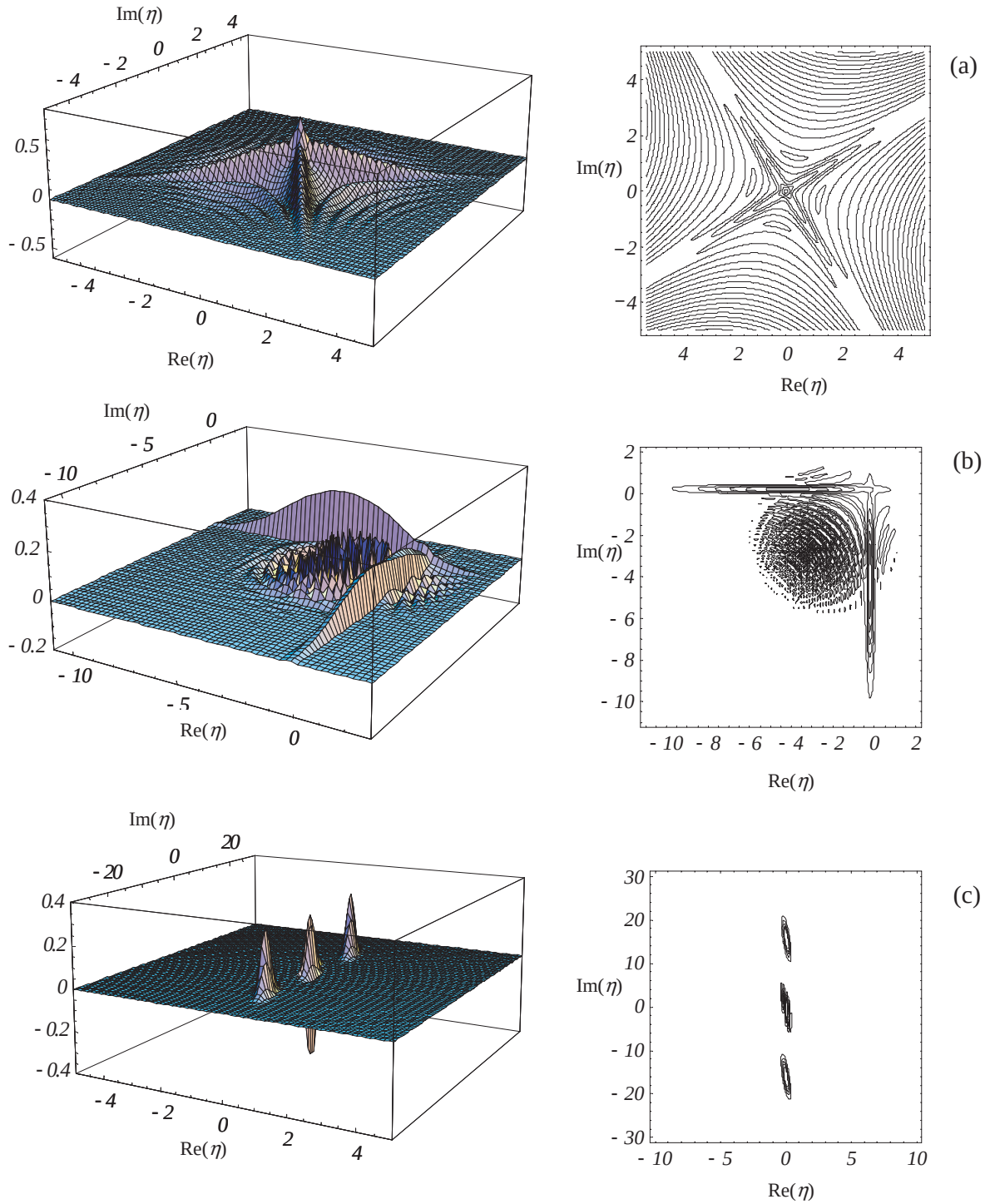

FIG. 2. (a) Wigner function obtained when $\Theta=\pi$, $\alpha=0$, $\kappa=\chi/20$, and $\chi\tau=2.06$. The variances for the quadrature operators read $\langle\Delta X_1\rangle=\langle\Delta X_2\rangle=2.63$ and the squeezing factor attained is $r(t_2)=1.45$. The mean photon number is 2.96. (b) Wigner function obtained when $\Theta=\pi$, $\alpha=\sqrt{2}$, $\kappa=\chi/20$, and $\chi\tau=3.99$. The variances for the quadrature operators read $\langle\Delta X_1\rangle=5.58$ and $\langle\Delta X_2\rangle=5.93$ and the squeezing factor is $r(t_2)=1.55$. The mean photon number is 26.38. (c) Wigner function obtained when $\Theta=0$, $\alpha=5$, $\kappa=\chi/20$, and $\chi\tau=1.68$. The variances for the quadrature operators read $\langle\Delta X_1\rangle=0.31$ and $\langle\Delta X_2^2\rangle=32.0$ and the squeezing factor is $r(t_2)=1.5$. The mean photon number is 256.17.

than those generated as circular states, i.e., a superposition of M coherent states having the same modulus and uniformly distributed around a circle in the phase space [35]. To do this, we have to pass N atoms through the cavity, obtaining the state defined in Eq. (32), where $M=2^N$. Remembering that $\Xi_k(t)=r_{\ell_1,\ldots,\ell_N}(t)\exp[i\varphi_{\ell_1,\ldots,\ell_N}(t)]$ and that the squeezing factor $r(t)$ does not depend on the atomic state, differently from the squeezing direction in phase space $\varphi_\ell(t)$, we

get $\Xi_k(t)=r(t)\exp[i\varphi_k(t)]$, where we have defined $\varphi_k(t)\equiv\varphi_{\ell_1,\ldots,\ell_N}(t)$, with k running from 1 to 2^N. With these considerations, we obtain from Eq. (32) the photon distribution function

$$\begin{aligned}\mathcal{P}_n(t)&=|\langle n|\Psi_N(t)\rangle|^2\\&=|\mathcal{N}_+\sum_{k=1}^{2^N}C_k(t)\langle n|S[\Xi_k(t)]|\vartheta_k(t)\rangle|^2\\&=|\mathcal{N}_+|^2\sum_{k,m=1}^{2^N}\frac{[\tanh r(t)]^n}{2^n n!\cosh r(t)}e^{i[\varphi_m(t)-\varphi_k(t)]n/2}\exp\left(-\frac{1}{2}(|\vartheta_k(t)|^2+|\vartheta_m(t)|^2)+\frac{1}{2}\tanh r(t)\{[\vartheta_k^*(t)]^2e^{i\varphi_k(t)}\right.\\&\left.+[\vartheta_m(t)]^2e^{-i\varphi_m(t)}\}\right)H_n^*\left(\frac{\vartheta_k(t)e^{-i\varphi_k(t)/2}}{\sqrt{2\cosh r(t)\sinh r(t)}}\right)H_n\left(\frac{\vartheta_m(t)e^{-i\varphi_m(t)/2}}{\sqrt{2\cosh r(t)\sinh r(t)}}\right),\end{aligned}\tag{52}$$

where $H_n(x)$ is the nth Hermite polynomial evaluated at x. We have assumed that all N atoms were prepared in the same state $(|0\rangle+|1\rangle)/\sqrt{2}$ and detected in their excited states.

In order to get the superposition of squeezed coherent states centered around the origin of the phase space (as required to generate the number state), we have to switch off the linear amplification process to obtain, from Eq. (12b), $\Lambda_\ell(t)=0$, leading to coherent states having equal amplitudes $\vartheta_k(t)\equiv e^{-i\beta_{\ell_1,\ldots,\ell_N}(t)}\theta_{\ell_1,\ldots,\ell_N}(t_i)=e^{-i\beta_k(t)}\alpha$. In addition, assuming α is real, we have to adjust $\beta_k(t)$ to $(1-k)\pi/N$ and $\varphi_k(t)=(k-1)2\pi/N$, to get a symmetric distribution of these states around the center of the phase space. With these adjustments [which are achieved through the interaction times between the N atoms and the cavity mode and also through the parametric amplification parameters $\kappa(t)$, $\eta(t)$] the photon distribution function simplifies to

$$\begin{aligned}\mathcal{P}_n(t)=|\mathcal{N}_+|^2&\sum_{k,m=1}^{2^N}\frac{[\tanh r(t)]^n}{n!\cosh r(t)}e^{-|\alpha|^2(1-\tanh r(t))}\\&\times\left[H_n\left(\frac{|\alpha|}{\sqrt{2\cosh r(t)\sinh r(t)}}\right)\right]^2\\&\times\sum_{k,m=1}^{2^N}e^{i[\varphi_m(t)-\varphi_k(t)]n/2}.\end{aligned}\tag{53}$$

In Fig. 3(a) we present the Wigner distribution function of the state generated from the passage of $N=2$ atoms through a cavity initially prepared in the coherent state $|\alpha|=7.4$ with $r=0.99$. These choices of the parameters $|\alpha|$ and r are considered in order to maximize the photon distribution function for $n=8$, attaining $\mathcal{P}_{n=8}(t)=0.95$, which is exactly the fidelity $|\langle 8|\Psi_{N=2}(t)\rangle|^2$ of the prepared state with respect to the number state $|8\rangle$. The value 0.95 is considerably larger than that computed without the parametric amplification process, when a circular state is generated with maximum fidelity 0.56 with respect to the number state $|8\rangle$. The fidelity 0.56 is computed from an initial coherent state $|\alpha|=2.83$. In Fig. 3(b) we plot the Wigner function of the state prepared from the passage of $N=3$ atoms through a cavity initially prepared in the coherent state $|\alpha|=8$ with $r=0.67$. Here we obtain the optimal value $\mathcal{P}_{n=16}(t)=0.99$, to be compared with the fidelity 0.79 computed when the amplification process is switched off and a circular state is prepared, from an initial coherent state $|\alpha|=3.95$.

Note that with the passage of N atoms though the cavity a family of number states is obtained: $|n=q2^N\rangle$ with $q=1,2,\ldots$. However, we stress that the fidelity of the prepared state decreases as the integer q increases. In Table I we present the states $|n=q2^3\rangle$ for some values of q, in order to compare the maximized fidelities computed from our model $[\mathcal{F}_q=|\langle n=q2^3|\Psi_{N=3}(t)\rangle|^2]$ with those derived from the circular states technique (F). We do not present the values of $|\alpha|$ and r used to calculated the fidelities.

We thus conclude that the atom–driven-field process is suitable for preparing number states with higher fidelity than those generated as circular states. Next we present another application of the states generated by the atom–driven-field interaction.

VIII. PREPARING LONG-LIVED MESOSCOPIC SUPERPOSITION STATES

Evidently, the squeezed superposition in Eq. (30) was ideally prepared. In a real engineering process the dissipative mechanisms of the cavity and the two-level atom, despite the fluctuations intrinsic to their interaction, must be taken into account. The complex calculations involved in the engineering of quantum states under realistic quantum dissipation and fluctuation conditions can be computed through the phenomenological-operator approach presented in Refs. [22,24]. However, in this paper we will not take into account the action of the reservoir during the preparation of the squeezed superposition (30). As usual, to estimate the decoherence time, we next consider that an ideally prepared state is submitted to the action of a quantum reservoir described by a collection of harmonic oscillators whose Hamiltonian is $H_R=\Sigma_k\hbar\omega_k b_k^\dagger b$. In addition, we will be interested in the action of a vacuum-squeezed reservoir at absolute zero; its initial density operator reads $\rho_R=\Pi_k S_k|0_k\rangle\langle 0_k|S_k^\dagger$, S_k being

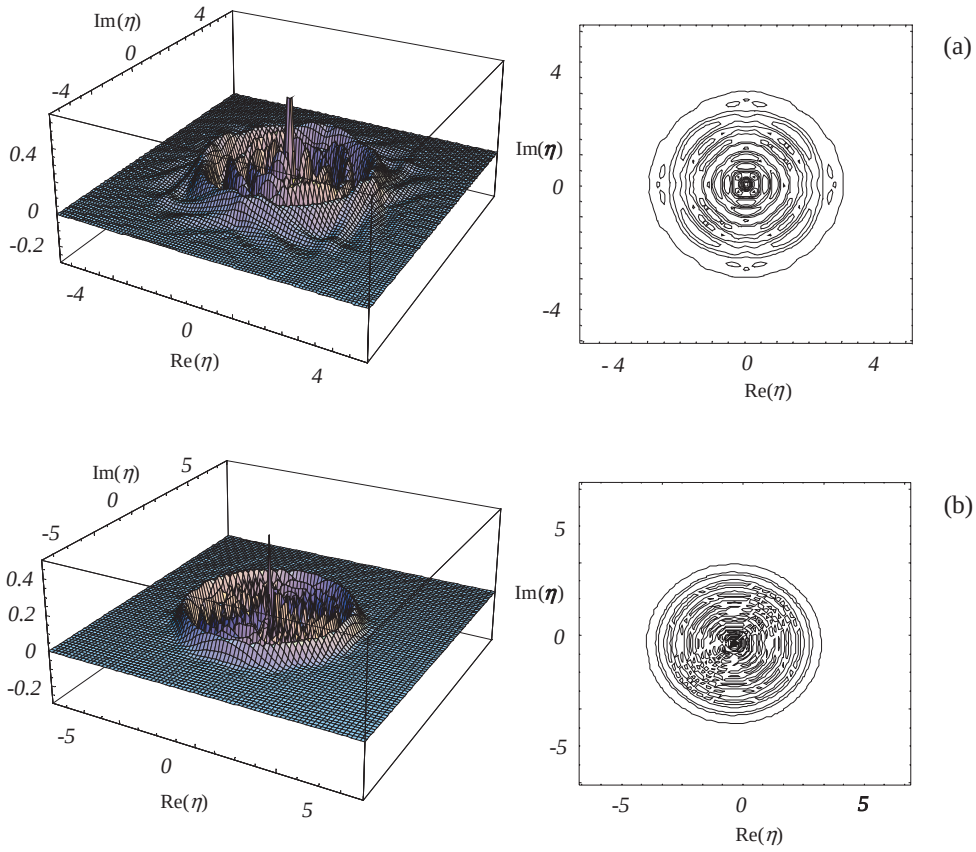

FIG. 3. (a) Wigner function of the state generated by passing $N=2$ atoms through a cavity initially prepared in the coherent state $|\alpha|=7.4$ with $r=0.99$, leading to the maximized photon distribution function $\mathcal{P}_{n=8}(t)=0.95$. (b) Wigner function of the state generated by passing $N=3$ atoms through a cavity initially prepared in the coherent state $|\alpha|=8$ with $r=0.67$, leading to the maximized photon distribution function $\mathcal{P}_{n=16}(t)=0.99$.

the squeezed operator for the kth bath oscillator mode. We are assuming here that, somehow, it is possible to describe all the mechanisms of dissipation of the cavity in terms of the action of a vacuum-squeezed reservoir. Describing the interaction between the reservoir and the system (the cavity mode modeled as $H_S=\hbar\omega a^\dagger a$) as $V=\Sigma_k\hbar(\lambda_k a^\dagger b_k+\lambda_k^* a b_k^\dagger)$, characterized by the strengths λ_k, the decoherence time deduced from the idempotency defect of the reduced density operator of the cavity field, as suggested in [51], is given by

$$\frac{\hbar^2}{2\tau^2}=-\langle H\rangle_{S,R}^2+\langle\langle H\rangle_S^2\rangle_R+\langle\langle H\rangle_R^2\rangle_S-\langle H^2\rangle_{S,R} \tag{54}$$

where the Hamiltonian comprehends a sum of three terms $H=H_S+H_R+V$. The average $\langle H\rangle_S(\langle H\rangle_R)$ is taken with respect to the density matrix of the system (reservoir), given by $\rho_S=|\Psi(t)\rangle\langle\Psi(t)|$ (ρ_R), where $|\Psi(t)\rangle$ is given by Eq. (30). From Eq. (54), the decoherence time of the cavity-field state is given by

$$\tau=\frac{\tau_R}{2|(2N+1)(\langle a^\dagger\rangle\langle a\rangle-\langle a^\dagger a\rangle)+2\,\mathrm{Re}\{M[\langle a^\dagger\rangle^2-\langle(a^\dagger)^2\rangle]\}-N|}, \tag{55}$$

where τ_R is the relaxation time defined by the cavity, $N=\sinh^2(\tilde{r})$, and $M=-e^{i\tilde{\varphi}}\sinh(2\tilde{r})/2$, $\tilde{r}$ and $\tilde{\varphi}$ being the squeeze parameters of the vacuum reservoir [33]. Here the mean values are computed from the prepared squeezed superposition (30). Since the excitation of the initial coherent state α and the squeeze parameters $(r(t_2),\varphi_\ell(t_2))$ have been fixed by the engineering protocol, we note that Eq. (55) depends only on the reservoir squeeze parameters $(\tilde{r},\tilde{\varphi})$. Considering the situation where α is real and $\langle\alpha|-\alpha\rangle=\exp(-2\alpha^2)\approx 0$ (implying $\alpha\approx\sqrt{2}$), in addition to the assumption that $\varphi_1(t_2)=\varphi$ and $\varphi_2(t_2)=\varphi+2n\pi$ (n integer) [implying $\Theta=|\varphi_1(t_2)-\varphi_2(t_2)|=2n\pi$, i.e., the states com-

TABLE I. The fidelity of the states $|\Psi_{N=3}(t)\rangle$ generated from our model ($\mathcal{F}_q$) and those derived from the standard circular states technique (F), for different values of the desired number states $|q2^3\rangle$.

q	$\mathcal{F}$	F
1	0.99	0.98
3	0.98	0.65
5	0.96	0.50
10	0.90	0.35

posing the superposition (30) are squeezed in the same direction], we obtain

$$\tau=\tau_R|1+\cosh(2\tilde{r})[2\alpha^2\cos\varphi\sinh(2r)-(1+2\alpha^2)\times\cosh(2r)]-\sinh(2\tilde{r})(1+2\alpha^2)\cos(\tilde{\varphi}-\varphi)\sinh(2r)-\alpha^2[\cos(\tilde{\varphi}-2\varphi)+\cos\tilde{\varphi}]\cosh(2r)+\alpha^2[\cos(\tilde{\varphi}-2\varphi)-\cos\tilde{\varphi}]|^{-1}, \quad (56)$$

where $r=r(t_2)$. The maximization of the decoherence time τ in Eq. (56) with respect to the parameters $(\tilde{r},\tilde{\varphi})$, leads to the results

$$\tilde{r}_A=r+\ln(1+4\alpha^2)/4, \quad \tilde{\varphi}_A=0, \quad (57a)$$

$$\tilde{r}_B=r-\ln(1+4\alpha^2)/4, \quad \tilde{\varphi}_B=\pi, \quad (57b)$$

which follow when we take $\varphi(t_2)=(2m+1)\pi$ and $\varphi(t_2)=2m\pi$ (m integer), respectively. When $\Theta\neq 2n\pi$, the maximum of τ turns out to be smaller than that for $\Theta=2n\pi$, given by either the pair $(\tilde{r}_A,\tilde{\varphi}_A)$ or $(\tilde{r}_B,\tilde{\varphi}_B)$. Observe that the directions of squeezing of both states composing the superposition (30), defined by the angles $\varphi_1(t_2)$ and $\varphi_2(t_2)$, has to be perpendicular to the direction of squeezing of the vacuum reservoir.

Next, we compute the ''distance'' in phase space between the centers of the quasiprobability distributions of the individual states composing the prepared superposition (30). This distance is defined by the quadratures of the cavity field $X=(a^\dagger+a)/2$ and $Y=(a-a^\dagger)/2i$, as

$$D=[(\langle X\rangle_2-\langle X\rangle_1)^2+(\langle Y\rangle_2-\langle Y\rangle_1)^2]^{1/2}, \quad (58)$$

the subscripts 1, 2 referring to the two states composing the superposition. Taking $\varphi_1(t_2)=\varphi_2(t_2)=(2m+1)\pi$ or $2m\pi$, the distance becomes $D=\langle X\rangle_2-\langle X\rangle_1=2\alpha\exp(r)$ or $2\alpha\exp(-r)$, respectively. We will focus on the case $\varphi_1(t_2)=\varphi_2(t_2)=(2m_1+1)\pi$, since it results in a large distance D between the two states composing what we actually want to be a mesoscopic superposition. The decoherence time and the mean photon number of the prepared state, obtained from the values $(\tilde{r}_A,\tilde{\varphi}_A)$, with $\exp(-2\alpha^2)\approx 0$, read

$$\tau\approx\tau_R/\alpha, \quad (59)$$

$$\langle n\rangle=\langle a^\dagger a\rangle\approx\alpha^2\exp(2r)+\sinh^2 r. \quad (60)$$

Remarkably, with the approximation $\exp(-2\alpha^2)\approx 0$, the decoherence time for the prepared cavity-field state when $\varphi_1(t_2)=\varphi_2(t_2)=(2m_2+1)\pi$—*under the action of a vacuum reservoir squeezed in the direction* $\tilde{\varphi}_A=0$—turns out to be practically independent of the parameter r and thus of its intensity $\langle n\rangle$ and distance D. Therefore, the decoherence time (59) becomes practically independent of the quantities that define the macroscopic character of the cavity-field state. From the result in Eqs. (59) and (60) we conclude that it is convenient to start from a coherent state α as small as possible [within the limit $\exp(-2\alpha^2)\approx 0$] and to adjust the macroscopic coupling parameter $|\mathfrak{P}_\ell|$ in order to obtain a large squeeze factor and, consequently, a large intensity of the prepared state and a large distance D, since we are actually interested in mesoscopic superpositions. We stress that, even considering the weak coupling regime ($|\mathfrak{P}_\ell|<1$), we obtain, from Eqs. (36a) and (42), large squeeze parameters: considering $|P_\ell|=0.1$, $\alpha=\sqrt{2}$, and the experimental running time about 2×10^{-4} s, we get a superposition state where $r\approx 2$ and $\langle n\rangle\approx 10^2$ photons.

The mechanism behind this result is the degree of entanglement between the prepared state and the modes of the reservoir, which depends on the relative direction of their squeezing, defined by the angles $\varphi_1(t_2)=\varphi_2(t_2)$ and $\tilde{\varphi}_A$. A result supporting this argument is presented in [52], where it is shown that the injection of two modes, squeezed in perpendicular directions, in a 50/50 beam splitter does not generate an entangled state. A careful analysis of the dependence of the relative direction of squeezing on the degree of entanglement between a prepared state and its multimode reservoir will be presented in [53]. Despite the fact that the mechanism behind the long-lived mesoscopic superpositions is mainly the perpendicular squeezing directions between the prepared state and the reservoir modes, the magnitude of the parameter r plays a crucial role in the present scheme for producing the mesoscopic superposition by increasing both its intensity $\langle n\rangle$ and distance D in phase space.

The values presented above for τ, $\langle n\rangle$, and D are to be compared with those when considering a nonsqueezed (NS) cavity-field state ($\langle n\rangle_{NS}=\alpha^2$, $D_{NS}=2\alpha$) under the influence of (i) a squeezed reservoir, resulting in the decoherence time $\tau_i\approx\tau_R/\alpha$, and (ii) a nonsqueezed reservoir, such that $\tau_{ii}\approx\tau_R/2\alpha^2$. Note that in both cases (i) and (ii) we obtain the ratios $\langle n\rangle/\langle n\rangle_{NS}\approx\exp(2r)$ and $D/D_{NS}\approx\exp(r)$. Therefore, despite the exponential increase in the ratios of both excitation and distance, we still get $\tau\approx\tau_i$ when comparing our results with previous schemes in the literature, where a squeezed reservoir is assumed for the enhancement of the decoherence time [54]; for nonsqueezed cavity-field states and reservoir, we obtain a still better result, $\tau\approx\alpha\tau_{ii}$.

IX. DISCUSSION AND CONCLUSION

We have presented a scheme for the preparation and control of a cavity-field state through atom–driven-field interaction. The Lewis and Riesenfield time-dependent invariants [48] were employed to obtain the eigenstates of the cavity mode dispersively interacting with a two-level atom and si-

multaneously under linear and parametric amplification processes. Protocols for preparing particular superposition states and the number state were presented. While relying on the manipulation of the initial states of the cavity mode and the two-level atom, considered in previous schemes [55], our protocol also employs the time-dependent parameters involved in the amplification sources to achieve particular superposition states and number states. We plotted some interesting ''Schrödinger cat''–like states and number states generated as circular squeezed states. We demonstrated that the number states generated as circular squeezed states exhibit higher fidelities than those generated as circular states.

We have shown how to prepare truly mesoscopic ''Schrödinger cat''–like states of the cavity field, actually squeezed superposition states, through their coupling to likewise squeezed reservoirs. When assuming that the squeezing direction of the cavity field is perpendicular to that of the reservoir modes, we found that the decoherence time of the prepared superposition state depends only on the initial coherent state of the cavity field from which the squeezed superposition is generated. Therefore, the decoherence time is independent of the average photon number and the distance in phase space between the centers of the quasiprobability distributions of the individual states composing the squeezed superposition. This result follows from the degree of entanglement between the prepared state and the modes of the reservoir, which depends on the relative direction of their squeezing. When the squeezing direction of the prepared superposition and that of the reservoir modes is perpendicular, the noise injected from the reservoir into the prepared cavity mode is minimized. A detailed analysis of the dependence of the relative direction of squeezing on the degree of entanglement between a prepared state and its multimode reservoir will be presented in [53].

The experimental implementation of the proposed scheme relies on the possibility of engineering a squeezed reservoir as well as of parametrically driving cavity-field radiation. We stress that a scheme to realize a squeezed bath physically for cavity modes, via quantum-nondemolition-mediated feedback, has already been presented in Ref. [56]. However, the feedback process in [56] does not eliminate the standard nonsqueezed bath and, as we have pointed out, our scheme requires an optimal squeezed-vacuum reservoir. The subject of quantum-reservoir engineering has attracted some attention, specially in the domain of trapped ions [25]; more specifically, a scheme has been presented for the engineering of squeezed-bath-type interactions to protect a two-level system against decoherence [27].

We emphasize that a proposal to implement the parametric amplification of an arbitrary radiation-field state previously prepared in a high-Q cavity is presented in Ref. [36]. As mentioned above, in this proposal the nonlinear process is accomplished through the dispersive interactions of a single three-level atom simultaneously with a classical driving field and a previously prepared cavity mode whose state we wish to squeeze. Moreover, regarding parametric amplification of cavity fields, a technique was recently suggested, based on pulsed excitation of semiconductor layers (on the cavity walls) by laser radiation [57]. It is worth mention that all the treatment developed above in the context of cavity quantum electrodynamics, for delaying the decoherence process of a squeezed superposition by coupling it to a vacuum-squeezed reservoir, can also be implemented in ion traps. We finally mention that the proposal presented here should motivate future theoretical and experimental investigations.

ACKNOWLEDGMENTS

We wish to express our thanks for the support of FAPESP (under Contract Nos. 99/11617-0, 00/15084-5, and 02/02633-6) and CNPq (Instituto do Milênio de Informação Quântica), Brazilian research funding agencies, and to Professor S. S. Mizrahi, Professor B. Baseia, Professor N. G. de Almeida, and Professor R. Napolitano for helpful discussions.

APPENDIX

In this appendix we present the Wigner function computed from Eq. (47) and the relation

$$\mathfrak{C}_S(\gamma,\gamma^*,t)=e^{|\gamma|^2/2}\mathfrak{C}_A(\gamma,\gamma^*,t)$$
$$=e^{|\gamma|^2/2}\langle\Psi(t)|e^{-\gamma^* a}e^{\gamma a^\dagger}|\Psi(t)\rangle, \quad \text{(A1)}$$

derived from the antinormal ordered characteristic function

$$\mathfrak{C}_A(\gamma,\gamma^*,t)=\mathrm{Tr}[\rho(t)\mathrm{e}^{-\gamma^* a}e^{\gamma a^\dagger}]$$
$$=\int\frac{d^2\beta}{\pi}|\langle\beta|\Psi(t)\rangle|^2 e^{-\gamma^*\beta+\gamma\beta^\dagger}, \quad \text{(A2)}$$

First we have to compute, from Eq. (30), the final cavity-field state $|\Psi(t)\rangle$, which, after a lengthy calculation, becomes

$$|\Psi(t)\rangle=|\Psi(t)\rangle=\mathcal{N}_+[c_1\Gamma_1(t)S(\varepsilon_1(t))|\theta_1(t)\rangle$$
$$+c_2\Gamma_2(t)S(\varepsilon_2(t))|\theta_2(t)\rangle], \quad \text{(A3)}$$

where the TD function $\Gamma_\ell(t)$ is defined in terms of that given by Eq. (19), as

$$\Gamma_\ell(t)=\Upsilon_\ell(t)\Upsilon_\ell(t_2)\Upsilon_\ell(t_1), \quad \text{(A4)}$$

and $\theta_\ell(t)$ is defined by Eq. (15). From Eqs. (A2) and (A3) we obtain, with $i,j=1,2$, the result

$$\mathfrak{C}_A(\gamma,\gamma^*,t)=\sum_{i,j=1}^{2}\frac{K_{ij}}{\sqrt{1-4b_ib_j^*}}\exp\left(\frac{(a_i+\gamma)(a_j^*+\gamma^*)+b_i(a_j^*-\gamma^*)^2+b_j^*(a_i+\gamma)^2}{1-4b_ib_j^*}\right), \quad \text{(A5)}$$

where the TD function K_{ij} reads

$$K_{ij}=|\mathcal{N}_+|^2 c_i c_j^* \Gamma_i(t)\Gamma_j^*(t)\,\mathrm{sech}[r(t)]\exp\left[-\frac{1}{2}[|\theta_i(t)|^2+|\theta_j(t)|^2]+\frac{1}{2}\tanh r(t)e^{i\varphi_i(t)}[\theta_i^*(t)]^2+e^{-i\varphi_j(t)}[\theta_j(t)]^2\right], \quad \text{(A6)}$$

and

$$a_i=\theta_i(t)\,\mathrm{sech}\, r(t), \quad \text{(A7)}$$

$$b_i=-\frac{1}{2}\tanh r(t)e^{i\varphi_i(t)}. \quad \text{(A8)}$$

Note that for the weak coupling regime, $r_1(t)=r_2(t)=r(t)$. Finally, from Eq. (47) and the characteristic function in Eq. (A5) we obtain the Wigner function

$$W(\eta,\eta^*,t)=\sum_{i,j=1}^{2}\frac{Aij}{\sqrt{B_{ij}^2-4C_{ij}D_{ij}}}\times\exp\left(\frac{C_{ij}E_{ij}^2+D_{ij}F_{ij}^2+B_{ij}E_{ij}F_{ij}}{B_{ij}^2-4C_{ij}D_{ij}}\right), \quad \text{(A9)}$$

where the TD functions A_{ij}, B_{ij}, C_{ij}, D_{ij}, E_{ij}, and F_{ij} satisfy

$$A_{ij}=\frac{K_{ij}}{\sqrt{1-4b_ib_j^*}}\times\exp\left[\frac{a_i(t)a_j^*(t)+a_i^2(t)b_j^*(t)+[a_j^*(t)]^2b_i(t)}{1-4b_i(t)b_j^*(t)}\right], \quad \text{(A10)}$$

$$B_{ij}=-\frac{1}{2}+\frac{1}{1-4b_i(t)b_j^*(t)}, \quad \text{(A11)}$$

$$C_{ij}=\frac{b_i(t)}{1-4b_i(t)b_j^*(t)}, \quad \text{(A12)}$$

$$D_{ij}=\frac{b_j^*(t)}{1-4b_i(t)b_j^*(t)}, \quad \text{(A13)}$$

$$E_{ij}=-\eta^*+\frac{2a_i(t)b_j^*(t)+a_j^*(t)}{1-4b_i(t)b_j^*(t)}, \quad \text{(A14)}$$

$$F_{ij}=\eta-\frac{2a_j^*(t)b_i(t)+a_i(t)}{1-4b_i(t)b_j^*(t)}. \quad \text{(A15)}$$

[1] M. Brune, E. Hagley, J. Dreyer, X. Maitre, A. Maali, C. Wunderlich, J. M. Raimond, and S. Haroche, Phys. Rev. Lett. **77**, 4887 (1996).

[2] C. Monroe, D. M. Meekhof, B. E. King, and D. J. Wineland, Science **272**, 1131 (1996)

[3] J. M. Raimond, M. Brune, and S. Haroche, Phys. Rev. Lett. **79**, 1964 (1997).

[4] S. Brattke, B. T. H. Varcoe, and H. Walther, Phys. Rev. Lett. **86**, 3534 (2001).

[5] M. Brune, F. Schmidt-Kaler, A. Maali, J. Dreyer, E. Hagley, J. M. Raimond, and S. Haroche, Phys. Rev. Lett. **76**, 1800 (1996).

[6] P. Knight, Nature (London) **380**, 392 (1996).

[7] C. Monroe, D. M. Meekhof, B. E. King, W. M. Itano, and D. J. Wineland, Phys. Rev. Lett. **75**, 4714 (1995).

[8] D. M. Meekhof, C. Monroe, B. E. King, W. M. Itano, and D. J. Wineland, Phys. Rev. Lett. **76**, 1796 (1996).

[9] D. Leibfried, D. M. Meekhof, B. E. King, C. Monroe, W. M. Itano, and D. J. Wineland, Phys. Rev. Lett. **77**, 4281 (1996).

[10] S. M. Barnett and D. T. Pegg, Phys. Rev. Lett. **76**, 4148 (1996); B. Baseia, M. H. Y. Moussa, and V. S. Bagnato, Phys. Lett. A **231**, 331 (1997).

[11] D. T. Pegg, L. S. Phillips, and S. M. Barnett, Phys. Rev. Lett. **81**, 1604 (1998); C. J. Villas-Bôas, Y. Guimarães, M. H. Y. Moussa, and B. Baseia, Phys. Rev. A **63**, 055801 (2001).

[12] G. M. D'Ariano, L. Maccone, M. G. A. Paris, and M. F. Sacchi, Fortschr. Phys. **48**, 599 (2000).

[13] P. G. Kwiat, K. Mattle, H. Weinfurter, A. Zeilinger, A. V. Sergienko, and Y. Shih, Phys. Rev. Lett. **75**, 4337 (1995).

[14] D. Bouwmeester, J. W. Pan, M. Daniell, H. Weinfurter, and A. Zeilinger, Phys. Rev. Lett. **82**, 1345 (1999).

[15] D. Bouwmeester, J.-W. Pan, K. Mattle, M. Eibl, H. Weinfurter, and A. Zeilinger, Nature (London) **390**, 575 (1997); D. Boschi, S. Branca, F. De Martini, L. Hardy, and S. Popescu, Phys. Rev. Lett. **80**, 1121 (1998); Y. H. Kim, S. P. Kulik, and Y. Shih, *ibid.* **86**, 1370 (2001); A. Furusawa, J. L. Sorensen, S. L. Braunstein, C. A. Fuchs, H. J. Kimble, and E. S. Polzik, Science **282**, 706 (1998).

[16] C. J. Villas-Bôas, N. G. de Almeida, and M. H. Y. Moussa, Phys. Rev. A **60**, 2759 (1999).

[17] R. M. Serra, C. J. Villas-Bôas, N. G. de Almeida, and M. H. Y. Moussa, J. Opt. B: Quantum Semiclass Opt. **4**, 316 (2002).

[18] J. I. Cirac, P. Zoller, H. J. Kimble, and H. Mabuchi, Phys. Rev. Lett. **78**, 3221 (1997); T. Pellizzari, *ibid.* **79**, 5242 (1997); H. J. Briegel, W. Dür, J. I. Cirac, and P. Zoller, *ibid.* **81**, 5932 (1998); S. J. van Enk, H. J. Kimble, J. I. Cirac, and P. Zoller, Phys. Rev. A **59**, 2659 (1999).

[19] J. I. Cirac and P. Zoller, Phys. Rev. Lett. **74**, 4091 (1995); Q.

A. Turchette, C. J. Hood, W. Lange, H. Mabuchi, and H. J. Kimble, *ibid.* **75**, 4710 (1995); I. L. Chuang, L. M. K. Vandersypen, X. Zhou, D. W. Leung, and S. Lloyd, Nature (London) **393**, 143 (1998); B. E. Kane, *ibid.* **393**, 143 (1998); L. M. K. Vandersypen, M. Steffen, G. Breyta, C. S. Yannoni, M. H. Sherwood, and I. L. Chuang, *ibid.* **414**, 883 (2001).

[20] W. H. Zurek, Phys. Today **44**(10), 36 (1991); W. H. Zurek and J. P. Paz, Phys. Rev. Lett. **72**, 2508 (1994).

[21] A. O. Caldeira and A. J. Leggett, Ann. Phys. (N.Y.) **149**, 374 (1983); Physica A **121**, 587 (1983).

[22] N. G. de Almeida, R. Napolitano, and M. H. Y. Moussa, Phys. Rev. A **62**, 033815 (2000); N. G. de Almeida, P. B. Ramos, R. M. Serra, and M. H. Y. Moussa, J. Opt. B: Quantum Semiclass. Opt. **2**, 792 (2000).

[23] R. Bonifacio, S. Olivares, P. Tombesi, and D. Vitali, Phys. Rev. A **61**, 053802 (2000).

[24] R. M. Serra, P. B. Ramos, N. G. de Almeida, W. D. José, and M. H. Y. Moussa, Phys. Rev. A **63**, 053813 (2001).

[25] J. F. Poyatos, J. I. Cirac, and P. Zoller, Phys. Rev. Lett. **77**, 4728 (1996); A. R. R. Carvalho, P. Milman, R. L. de Matos Filho, and L. Davidovich, *ibid.* **86**, 4988 (2001).

[26] A. R. R. Carvalho, P. Milman, R. L. de Matos Filho, and L. Davidovich, Phys. Rev. Lett. **86**, 4988 (2001).

[27] N. Lutkenhaus, J. I. Cirac, and P. Zoller, Phys. Rev. A **57**, 548 (1998).

[28] G. S. Agarwal, M. O. Scully, and H. Walther, Phys. Rev. Lett. **86**, 4271 (2001).

[29] C. J. Myatt, B. E. King, Q. A. Turchette, C. A. Sackett, D. Kielpinski, W. M. Itano, C. Monroe, and D. Wineland, Nature (London) **403**, 269 (2000).

[30] J. I. Cirac, Nature (London) **413**, 375 (2001).

[31] D. A. R. Dalvit, J. Dziarmaga, and W. H. Zurek, Phys. Rev. A **62**, 013607 (2000)

[32] C. K. Law and J. H. Eberly, Phys. Rev. Lett. **76**, 1055 (1996); F. L. Li and S.Y. Gao, Phys. Rev. A **62**, 043809 (2000).

[33] M. O. Scully and S. Zubairy, *Quantum Optics* (Cambridge University Press, Cambridge, England, 1997); D. F. Walls and J. Milburn, *Quantum Optics* (Springer-Verlag, Berlin, 1994).

[34] V. V. Dodonov, J. Opt. B: Quantum Semiclass. Opt. **4**, R1 (2002).

[35] J. Janszky, P. Domokos, and P. Adam, Phys. Rev. A **48**, 2213 (1993).

[36] C. J. Villas-Bôas, N. G. de Almeida, R. M. Serra, and M. H. Y. Moussa, quant-ph/0303119.

[37] R. E. Slusher *et al.*, Phys. Rev. Lett. **55**, 2409 (1985).

[38] R. M. Shelby *et al.*, Phys. Rev. Lett. **57**, 691 (1986).

[39] L. A. Wu *et al.*, Phys. Rev. Lett. **57**, 2520 (1986).

[40] P. Meystre and M. S. Zubairy, Prog. Allergy **89A**, 390 (1982); J. R. Kuklinski and J. L. Madajczyk, Phys. Rev. A **37**, R3175 (1988); M. Hillery, *ibid.* **39**, 1556 (1989).

[41] L. Davidovich, A. Maali, M. Brune, J. M. Raimond, and S. Haroche, Phys. Rev. Lett. **71**, 2360 (1993).

[42] J. M. Raimond, M. Brune, and S. Haroche, Rev. Mod. Phys. **73**, 565 (2001).

[43] M. J. Holland, D. F. Walls, and P. Zoller, Phys. Rev. Lett. **67**, 1716 (1994).

[44] H. J. Carmichael, G. J. Milburn, and D. F. Walls, J. Phys. A **17**, 469 (1984).

[45] S. S. Mizrahi, M. H. Y. Moussa, and B. Baseia, Int. J. Mod. Phys. B **8**, 1563 (1994).

[46] A. F. R. de Toledo Piza, Phys. Rev. A **51**, 1612 (1995).

[47] M. Zahler and Y. Ben Aryeh, Phys. Rev. A **43**, 6368 (1991).

[48] H. R. Lewis and W. B. Riesenfeld, J. Math. Phys. **10**, 1458 (1969).

[49] R. R. Puri and S. V. Lawande, Phys. Lett. **70A**, 69 (1979).

[50] B. Baseia, M. H. Y. Moussa, and V. S. Bagnato, Phys. Lett. A **231**, 331 (1997).

[51] Ji Il Kim, M. C. Nemes, A. F. R. de Toledo Piza, and H. E. Borges, Phys. Rev. Lett. **77**, 207 (1996).

[52] M. S. Kim, W. Son, V. Buzek, and P. L. Knight, Phys. Rev. A **65**, 032323 (2002).

[53] C. J. Villas-Bôas, R. M. Serra, and M. H. Y. Moussa (unpublished).

[54] M. S. Kim and V. Buzek, Phys. Rev. A **47**, 610 (1993).

[55] M. Brune *et al.*, Phys. Rev. A **45**, 5193 (1992).

[56] P. Tombesi and D. Vitali, Phys. Rev. A **50**, 4253 (1994).

[57] G. Carugno (private communication).